States in ^{13}C via Neutron Polarization Investigations for the ^{9}Be$(\alpha, n)^{12}$C Reaction*

D. C. De Martini,† C. R. Soltesz,‡ and T. R. Donoghue
Department of Physics, The Ohio State University, Columbus, Ohio 43210
(Received 22 December 1972)

Angular distributions of the neutron polarization for the ^{9}Be$(\alpha, n_0)^{12}$C and ^{9}Be$(\alpha, n_1)^{12}$C* (4.43-MeV) reactions have been measured at six projectile energies in the 4.5- to 5.85-MeV interval. Large polarizations are observed for both neutron groups over the whole energy range, making both groups useful sources of polarized neutrons. The ground-state neutron-polarization angular distributions have been analyzed simultaneously with the recent cross-section data of Obst *et al.* using an S-matrix search code to make J^{π} assignments to states in ^{13}C in the 13- to 15-MeV excitation energy range. The combined data set can be adequately described over the whole energy range by assuming the presence of at least five broad states. The J^{π} assignments and the probable excitation energies for these states are given.

I. INTRODUCTION

This paper reports observations and analyses of neutron polarizations in the ^{9}Be$(\alpha, n)^{12}$C reaction for the 4- to 6-MeV α-energy interval. The motivations for the experimental investigations were (1) to provide information of a new kind in this energy interval relating to the reaction mechanism, (2) to utilize these data along with published cross-section data to obtain spectroscopic information, and (3) to determine if this reaction is a useful source of higher-energy polarized neutrons.

Previous investigations of this reaction employing several experimental techniques have resulted in conflicting interpretations of the reaction mechanism involved, ranging from a purely compound-nucleus picture to one where a pure direct reaction including a heavy-particle-stripping process is advocated. Lietz *et al.*[1] discuss most of the relevant work on this point. It is clear however that the compound-nucleus mode is important as the cross-section excitation curves exhibit pronounced fluctuations up to $E_{\alpha} = 12$ MeV. Much of our knowledge of states in the ^{13}C compound system for $E_x > 11$ MeV has been obtained from these (α, n) investigations. However, the observed structure is generally broad with an occasional sharp peak superimposed on this, and it is likely that more than one level contributes to the individual fluctuations.[2,3] An analysis of reaction cross-section data alone would be difficult, and probably inconclusive; in fact, there are very few attempts reported in the literature. As might be expected, our knowledge of the ^{13}C level structure in the 10–20-MeV excitation range is largely unknown.[4]

It is in situations such as this that supplementary experimental information such as provided by polarization investigations can be of considerable value. For instance, the measurement of complete polarization angular distributions over a broad energy interval can aid in establishing the reaction mechanism. An analysis of $\sigma(\theta)$ and $P(\theta)$ data simultaneously can provide useful spectroscopic information, as shown by Darden[2] and Baker *et al.*[5] In the present work the ground-state neutron-polarization data provide evidence supporting the dominance of a compound-nucleus mechanism. Accordingly our $P(\theta)$ data have been analyzed together with published $\sigma(\theta)$ data[6] to make a number of spin and parity assignments to states in ^{13}C. Our measurements confirm much of the earlier experimental work reported by Lietz *et al.*[1] for lower energies and the analysis of their data reported by Darden.[2] In both the present analysis and in that reported by Darden, an S-matrix search code was used to determine those matrix elements that provided the best simultaneous description of the $\sigma(\theta)$ and $P(\theta)$ data.

The ^{9}Be$+\alpha$ elastic scattering process has recently been studied at this laboratory by Goss *et al.*[7] for the same energy interval. These authors carried out an R-matrix analysis of their data in the 3.5- to 5.0-MeV energy interval, using assignments derived in the (α, n_0) analyses as a starting point. The results of their work are reported in the following paper.

As noted above, another motivation for the present investigation centers around the favorable qualities of this reaction as a source of polarized neutrons. The reaction has a large Q value (+5.71 MeV for the ground-state transition), the cross sections are large at some angles and energies, and the separation of the states in the final nucleus is sufficient for the contributions from each of the neutron groups to be easily separated. These factors, together with some of the high polarizations observed in this work, combine to make this reaction the first potentially useful source in the 4- to 10-MeV neutron energy range available to

users of single-ended electrostatic accelerators. Because this reaction was previously reported by Lietz *et al.* to be such a useful source at $E_\alpha = 2.65$ MeV, a reinvestigation of that energy was also made. Polarizations higher than reported by those authors were found, making this an even more useful source at this energy.

II. EXPERIMENTAL METHOD

The polarization of the neutrons was determined by measuring the asymmetry in the scattering of the neutrons from helium using the apparatus illustrated schematically in Fig. 1. Neutrons emitted in the reaction at a lab angle θ_1 traverse the axis of a solenoid that is used to rotate the polarization vector of the neutron beam through ±90°. This technique originally proposed by Hillman, Stafford, and Whitehead[8] interchanges the roles of the counters used in the asymmetry measurements without a physical exchange being made. The neutrons are then scattered from a high-pressure helium-gas scintillator into either of two plastic neutron detectors located at $\theta_2 = 123°$(lab). A fast coincidence requirement between the helium scintillator and one of the two neutron detectors is used to gate a multichannel pulse-height analyzer whose linear input is a signal from the helium scintillator. Contributions to the pulse-height spectrum from the various neutron groups can be easily separated and used in the determination of the asymmetry. Although this apparatus has been used for a number of experiments,[5,9-11] the major components of the system have not been discussed before and are accordingly presented in some detail below.

A. Neutron Polarimeter

The air-core solenoid was constructed of 1512 turns of 0.64-cm square Cu tube in a modular design consisting of three coils with 12 pancakes per coil. The magnet which is 53 cm long, 35.5 cm o.d., and 5.1 cm bore is completely encased in a soft iron box with 2.5-cm-thick walls to reduce fringe fields. With the modular design, the magnet may be shortened to permit investigations of low-yield reactions where a short target-to-second-scatterer distance is desirable. The solenoid is powered by a 33-kW motor generator (MG) to produce a maximum axial field of 10 kG, permitting 20-MeV neutrons to be precessed through 90°. The output current of the MG set is stabilized to 0.1% by a solid-state control circuit,[12] which also permits accurate and automatic reversal of the current through the solenoid in approximately 20 sec. During the measurements, the current was reversed at 5-min intervals to reduce effects due to possible drifts in the detection electronics. The solenoid is positioned on a track mounted on top of a table. The latter can be pivoted to any reaction angle back to 135°(lab) to within 0.2°. The track permits flexibility in selecting the source-to-scatterer distance.

The helium scintillator is shown in detail in Fig. 2 and is qualitatively similar to that of Shamu.[13]

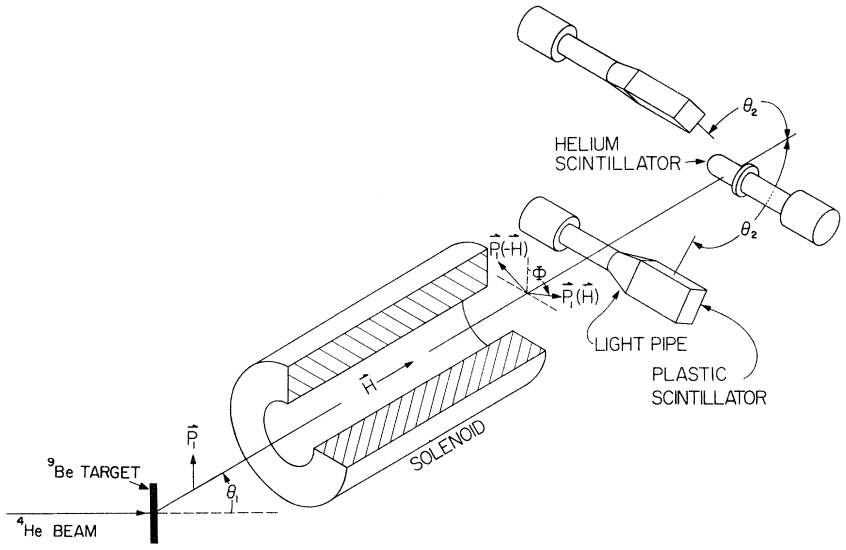

FIG. 1. A schematic view of the neutron polarimeter. The vector $\vec{P}_1$ represents the neutron polarization before and after precession by the solenoid through the angle $\pm\Phi$ where $\Phi \simeq 90°$.

Briefly, the scintillator was prepared by highly polishing the inner surface, coating this surface first with a thin layer of Al and then a thick layer of MgO, baking out the whole cell under high vacuum, and finally depositing by evaporation a wavelength shifter, *pp'*-diphenylstilbene (DPS) on top of the MgO. In an effort to construct a scintillator with improved energy resolution ($\Delta E/E$), it was observed that the resolution and the light output from any local region of the scintillator was strongly dependent on the DPS thickness in that region. Therefore, a study of the optimum distribution of the wavelength shifter was made. For this study the scintillator was pressurized to ~30 atm with a helium-xenon gas mixture and then irradiated with a well-collimated (1-cm-square) neutron beam. Gated helium recoil spectra (e.g., see Fig. 3) were recorded for each irradiation of the different regions of the cell where the detector geometries and fast-coincidence requirements were the same as those used in the asymmetry measurements described below. After noting variations in ($\Delta E/E$) and/or in the centroid channel of the gated recoil peak, a new distribution for the DPS was determined from empirical observations and another evaporation was made. By repeating this procedure several times, an over-all energy resolution[14] for the scintillator of 5% full width at half maximum (FWHM) for polonium-α particles and of ~10% for 5-MeV incident neutrons was obtained. This resolution is approximately twice as good as that obtained for other helium cells used in polarization measurements. The improvement noted here appears to be due to both the compensating distributions as well as to the increased thickness of the DPS layer. This thickness was calculated to vary from 0.7 to 2.95 mg/cm^2 over the cell volume. We have constructed several scintillators over the past few years with similar results. We have made no attempts at improving the resolution further because of the fragile nature of the MgO layer. We have not noticed any gas poisoning over a six month interval, which may be due to our extensive bakeout prior to the DPS evaporation. For the polarization measurements, the scintillator was pressurized with a purified mixture of helium (152 atm) and xenon (8 atm). The 5% xenon contribution was found to maximize the light output of the scintillator. The soft iron pipe noted in Fig. 2 was used to eliminate gain shifts in the photomultiplier tube induced by the solenoid or other stray magnetic fields.

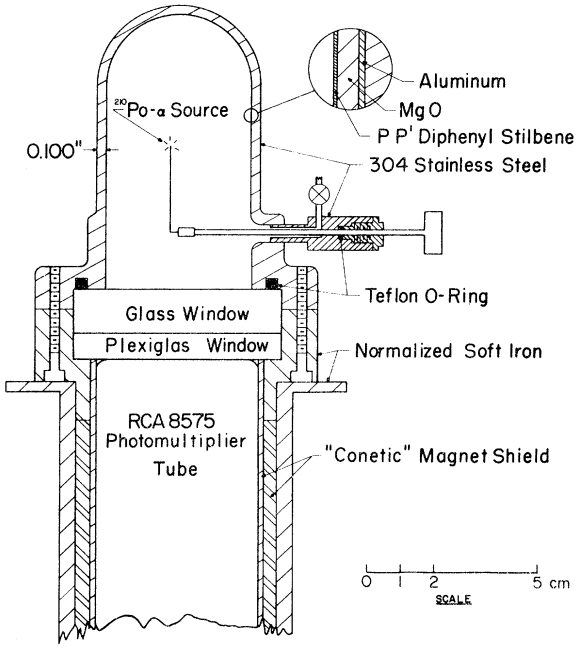

FIG. 2. A detailed view of the high-resolution helium-gas scintillator used in the polarization measurements. Fabrication details are discussed in the text.

B. Experimental Procedure

A 4- to 10-μA beam of α particles from the Ohio State University 6-MV Van de Graaff acceler-

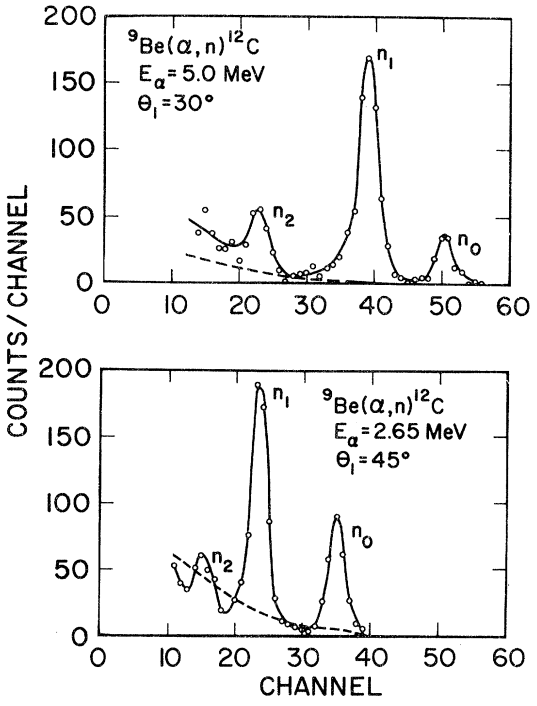

FIG. 3. Two typical gated pulse-height spectra, illustrating the separation of the various neutron groups. The dashed line sketched here indicates the background that has been subtracted.

ator struck a Be target after being magnetically analyzed to an energy resolution of 0.15%. The targets were prepared by vacuum evaporation of Be onto a 3-cm-diam tungsten disk, 0.5 mm thick. The target thicknesses were obtained from a measurement of the threshold rise curve in the ^{9}Be-$(p,n)^9$B reaction and were on the average 300 keV thick for 5-MeV α particles, although several measurements were made using targets between 105 and 460 keV thick. The thicknesses were also determined by weighing techniques with consistent agreement to 5% between the two measurements. To prevent target deterioration under bombardment, the target assembly was continuously rotated and cooled with distilled water. The target assembly also served as a Faraday cage for the beam which was collected and fed into a precision current integrator that was used for normalization purposes.

A brass collimator placed in the bore of the solenoid restricted the neutron flux to a cone of half angle 1.5°. After traversing the central axis of the magnet, the neutrons struck the helium scintillator positioned 90 cm from the target and were elastically scattered at 123°(lab) by the helium into either of two Pilot-B plastic scintillators 5.1 cm (in $\Delta\phi$), 2.54 cm (in $\Delta\theta$), and 5.1 cm deep, positioned 15 cm from the central axis. A fast coincidence was required ($2\tau = 12$ nsec) between the helium cell and either of the plastic scintillators. This pulse was used (1) to gate a multichannel pulse-height analyzer, whose input was a linear signal from the helium scintillator, and (2) to route this linear signal into one of four quadrants of the analyzer, depending on whether the neutron was scattered up or down (see Fig. 1) and on whether the neutron spins were precessed clockwise or counterclockwise by $\pi/2$. A recent version of the electronics used is given by Baker *et al.*[5] Two typical gated helium-recoil spectra are shown in Fig. 3 where the measured backgrounds have been subtracted. The neutron transitions to the three lowest states are well separated, permitting simultaneous measurements for n_0 and n_1 in most instances. Nonsubtracting background contributions to the n_2 group at other angles prevented reliable polarization measurements for this group.

Background contributions to the recoil spectra may result from accidental coincidence events or from true coincidences initiated by neutrons not coming directly from the target. The first source was measured by inserting an extra delay of 100 nsec in the helium signal input to the fast-coincidence circuit. The second source was determined by inserting a solid brass bar of negligible transmission (<1%) in the bore of the solenoid. These backgrounds were measured for $\frac{1}{3}$ to $\frac{1}{2}$ of the total integrated beam charge of the foreground runs and either at alternate reaction angles or at every angle when they were comparatively large. The contributions from these two sources were roughly equal. Total backgrounds for the n_0 group typically varied from 3–20% of the total counts accumulated and for the n_1 group from 2–8%. For a few of the n_0 data points, the total backgrounds were as high as 38% when the reaction cross section was near minimum.

The polarization of each group of neutrons was calculated by integrating the counts in its associated peak in the net helium-recoil spectrum corresponding to neutrons scattering into the top (T) and bottom (B) detectors for each ($\pm$) sense of the solenoid current. The asymmetry ratio r was then calculated as the geometric mean of the individual detector ratios by the expression

$$r = \left(\frac{T_+}{T_-} \times \frac{B_-}{B_+} \right)^{1/2} .$$

The asymmetry $e = P_1 P_2$ can be determined from r by

$$e = \frac{r-1}{r+1} .$$

P_1 is the polarization of the neutrons emitted in the reaction for an unpolarized incident beam and P_2 is the analyzing power for elastic n-α scattering. The Basel convention is used in computing the sign of the polarization. The use of a precession magnet and two neutron detectors in the vertical plane combined with this manner of data reduction eliminates all known sources of instrumental asymmetries.

The average value of the analyzing power of helium, $\langle P_2 \rangle$, over the experimental geometry was calculated using the phase shifts of Satchler *et al.*[15] The computed average[14] included an integration over the volume of the gas scintillator and the in-plane (θ_2) and azimuthal (ϕ_2) angles associated with the plastic neutron detector. Each element of the integration was weighted by the helium differential cross section as a function of angle and energy and by the plastic detector efficiency as a function of the neutron energy and the geometry subtended by the detector. The averaged values of the analyzing power for helium ranged from 0.76 to 0.95 in these measurements.

In most cases, simultaneous measurements on n_0 and n_1 were made. Generally, the n_1 group of neutrons was precessed through $\pi/2$, necessitating a correction to the asymmetry for the n_0 group. This correction increased the measured asymmetry by a factor averaging 1.05, but was 1.12 in the worst case. Depolarization effects

TABLE I. $^{9}Be(\alpha, n_0)^{12}C$ and $^{9}Be(\alpha, n_1)^{12}C^*$ (4.43-MeV) neutron polarizations.

Lab angle (deg)	Energy (MeV) 4.5	4.75	5.0	5.25	5.50	5.85
			Ground-state group			
15	−0.20 ± 0.04	−0.15 ± 0.08	−0.49 ± 0.06	−0.44 ± 0.04	−0.36 ± 0.04	−0.15 ± 0.06
30	−0.24 ± 0.04	−0.21 ± 0.05	−0.53 ± 0.07	−0.44 ± 0.03	−0.33 ± 0.03	−0.04 ± 0.05
45	−0.17 ± 0.07	+0.11 ± 0.06	−0.47 ± 0.07	−0.26 ± 0.04	−0.03 ± 0.04	+0.24 ± 0.07
52.5				+0.05 ± 0.05	+0.23 ± 0.05	
60	+0.45 ± 0.04	+0.30 ± 0.08	+0.09 ± 0.07	+0.30 ± 0.06	+0.52 ± 0.04	+0.52 ± 0.07
75	+0.28 ± 0.08	+0.29 ± 0.07	+0.13 ± 0.08	+0.09 ± 0.10	+0.11 ± 0.10	+0.63 ± 0.16
90	+0.11 ± 0.05	+0.01 ± 0.04	+0.06 ± 0.07	+0.02 ± 0.11		
105	−0.11 ± 0.04	−0.13 ± 0.04	+0.21 ± 0.10	+0.47 ± 0.04	+0.52 ± 0.05	+0.04 ± 0.06
120	−0.16 ± 0.04	−0.31 ± 0.04	+0.18 ± 0.13	+0.66 ± 0.04	+0.55 ± 0.04	+0.42 ± 0.06
130	+0.05 ± 0.04	+0.07 ± 0.05	+0.10 ± 0.19	+0.19 ± 0.06	+0.48 ± 0.05	+0.59 ± 0.05
			First-excited-state group (4.43 MeV)			
15	+0.06 ± 0.02	+0.05 ± 0.02	−0.05 ± 0.02	−0.09 ± 0.02	−0.14 ± 0.02	−0.09 ± 0.02
30	+0.06 ± 0.02	+0.04 ± 0.02	−0.09 ± 0.02	−0.07 ± 0.02	−0.20 ± 0.02	−0.18 ± 0.02
45	−0.05 ± 0.02	−0.04 ± 0.02	−0.10 ± 0.02	−0.04 ± 0.02	−0.12 ± 0.02	−0.06 ± 0.02
52.5				+0.01 ± 0.02	−0.04 ± 0.02	
60	−0.16 ± 0.02	−0.13 ± 0.02	−0.07 ± 0.02	+0.02 ± 0.02	−0.01 ± 0.02	+0.05 ± 0.02
67.5					−0.04 ± 0.02	
75	−0.26 ± 0.02	−0.28 ± 0.02	−0.18 ± 0.02	−0.12 ± 0.02	−0.10 ± 0.02	−0.08 ± 0.02
90	−0.36 ± 0.02	−0.31 ± 0.02	−0.25 ± 0.02	−0.30 ± 0.02		
105	−0.33 ± 0.02	−0.35 ± 0.02	−0.27 ± 0.02	−0.34 ± 0.02	−0.24 ± 0.02	−0.10 ± 0.02
120	−0.28 ± 0.02	−0.27 ± 0.02	−0.14 ± 0.02	−0.25 ± 0.02	−0.23 ± 0.02	−0.17 ± 0.02
130	−0.21 ± 0.02	−0.22 ± 0.02	+0.06 ± 0.02	−0.17 ± 0.02	−0.24 ± 0.02	−0.19 ± 0.02

may arise from magnetic field components in the solenoid that are not parallel to the neutron-momentum direction. An estimation of this from the work of Atkinson and Sherwood[16] shows that the corrections should be less than 1% for the present solenoid configuration and hence can be neglected.

III. EXPERIMENTAL RESULTS

The polarizations measured for the ground-state (g.s.) and the first-excited-state (f.e.s.) neutron groups in the $^{9}Be(\alpha, n)$ reaction are listed in Table I as a function of the average ^{4}He energy and of the neutron emission angle in the laboratory system. The quoted uncertainties arise principally from statistical considerations. The data are also plotted in Fig. 4, where a smooth solid curve has been sketched through the data points. Sizable polarizations are observed in all angular distributions for both neutron groups which, as will be discussed below, makes this reaction a useful source of polarized neutrons at some energies and angles. The g.s. polarization angular distributions exhibit a shape that changes with energy in a manner that would be expected if the reaction proceeds predominantly through broad compound-nuclear states. The f.e.s. distributions on the other hand show much less variation with energy, suggesting that a direct-reaction mechanism may be of some importance here.

A comparison of our results with those of Lietz *et al.*[1] can be made at 4.5 MeV. At their angles of measurement (15, 30, and 120°) for the g.s. group, the agreement between the two sets of data is well within statistics. However, their f.e.s. group measurements, which are indicated by the dashed line in Fig. 4, are consistently lower than the values determined in the present work. In an attempt to explain this discrepancy, we note that a number of advances in the technology of fast electronics and of constructing high-resolution helium-gas scintillators took place in the time between the two experiments. For instance, the gated helium-recoil peaks for the g.s. and f.e.s. neutron groups were completely separated in our spectra so that no contamination of the peaks from other neutron groups was possible. In the work of Lietz *et al.* the energy resolution appears to be 2 to 3 times worse than employed in the current work and this necessitated some peak-fitting procedures to eliminate contributions due to overlapping peaks. The present measurements at this energy were

made with the neutron spins fully precessed through $\pm\pi/2$, whereas Lietz *et al.* had to correct their data appreciably for inadequate spin precession. Furthermore, in a repeat of Lietz *et al.* work at 2.65 MeV (discussed below), it was noted that their reported values were also low compared to the present results. A recent measurement by Stammbach *et al.*[17] at this same energy has substantiated the higher values reported previously by our group.[18]

A contour plot of the polarization for the g.s. transition is shown in Fig. 5 where lines of constant polarization in 0.1 increments are sketched as a function of $\theta_{c.m.}$ and $E(^4\text{He})$. Also sketched above the contour map is a 0° cross-section excitation curve measured by Obst, Grandy, and Weil.[6] The arrows on this curve indicate the energies at which polarization angular distributions were measured. In this plot, several closed contours are noted which can be correlated with the structure in the $\sigma(0°)$ curve, a correlation[10] which suggests that compound-nuclear effects are present in this reaction. Consequently, an attempt has

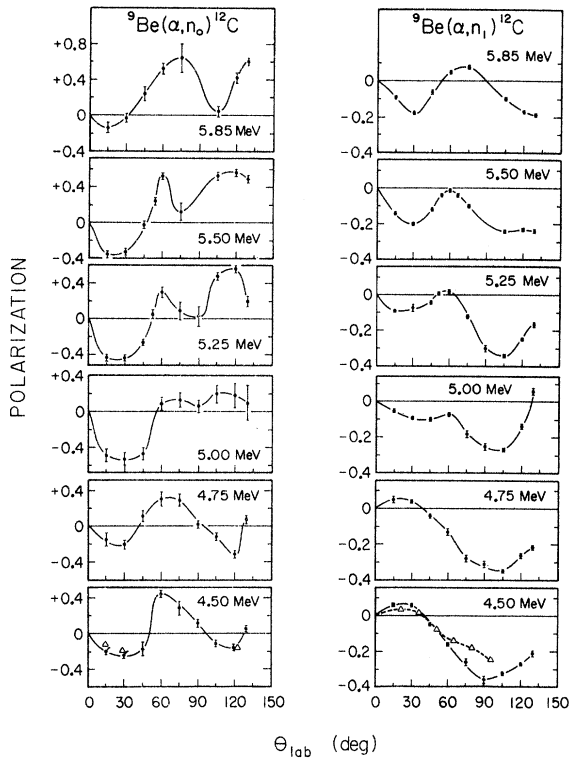

FIG. 4. The polarizations measured for the g.s. and f.e.s. neutron groups plotted for the various energies of measurement. The solid line is sketched in as an aid to the eye. The Δ's plotted at E_α=4.5 MeV are the data of Lietz *et al.* (Ref. 1) which are directly comparable to our results.

been made to analyze $P(\theta)$ data together with $\sigma(\theta)$ data of Obst, Grandy, and Weil in terms of states in ^{13}C and this will be discussed in the following section. A contour plot (not shown) constructed for the f.e.s. neutron group, on the other hand, showed little structure and no correlation patterns with $\sigma(0°)$ were noted. Furthermore, Van der Zwan and Geiger[19] note that the magnitude of the cross section for the f.e.s. transition is so large that a surface reaction surely is an important contribution in this channel. As our analysis program could not take this second reaction mode into consideration, no analysis of these data has been attempted at this time.

IV. REACTION ANALYSIS

The polarization data for the g.s. transition were analyzed simultaneously with the differential cross-section data under the assumption that the compound-nucleus mode completely dominates this transition. The analysis was carried out using the S-matrix search code of Marr[20] in which $\sigma(\theta)$ and $P(\theta)$ are calculated from the amplitudes and phases of the matrix elements corresponding to levels of definite J^π in the ^{13}C compound system. The general expressions for $\sigma(\theta)$ and $P(\theta)$ as given by Welton[21] are used. The program uses a direct search routine to obtain the best simultaneous fit to the $\sigma(\theta)$ and $P(\theta)$ data at each energy for each group of matrix elements S^{J^π} $(s'l'\alpha'; sl\alpha)$ tried as likely candidates for the contributing states of J^π in ^{13}C. With such an analysis,[5] J^π assignments can be made to states even when little is known *a priori*. This is particularly true when the states are broad and overlapping, since the derived matrix elements must exhibit a smooth energy dependence that resembles the structure in the excitation curves. This type of analysis was used earlier by Lietz, Trevino, and Darden[1,2] in their analysis of this reaction at lower energy and by Baker *et al.*[5] in the ^{13}C$(\alpha, n)^{16}$O reaction analysis. Operational details of the computer code are given by Marr[20] and by Baker *et al.*[5] The latter also discuss some of the difficulties in carrying out a "conventional" R-matrix analysis when little is known about the contributing states.

The recent summary[4] of the ^{13}C level structure shows that little is known about the states at excitation energies above 12 MeV. Because the structure in the (α, n) cross-section excitation curves is generally broad, the number of states participating in the reaction may be much greater than the number of bumps. To keep the analysis within manageable proportions in this situation, we have made several restrictive assumptions. The number of levels that may be important contribu-

tors at a given energy is limited to four. Although this may seem large at first, the states are broad and overlapping[4] and hence may be expected to influence the data several level widths away, particularly the polarization data. In addition, each state of definite J^π may be formed by two values of incoming orbital angular momentum l_α whereas, in the outgoing channel, the orbital angular momentum is unique for the g.s. transition. The states are accordingly labeled by the convention J^π (l_α). For computational reasons the two l_α possibilities must be treated as separate levels. It was assumed that one of the two l_α values dominated in the reaction for a given state, with each being tried separately. In a few cases, both l_α values were included in the calculation. Levels with $l_\alpha \geq 5$ units were not considered. Obviously not all combinations of levels (or l_α values) could be tried, nor could a dependency on the trial parameters for the S matrix elements used in the search code be explored for every case. The latter was tried in most of the more plausible calculations. In our search for alternate sets of levels, parameters derived in a calculation that yielded a particularly good fit at one energy were always used as input for similar calculations at neighboring energies. In this way, it was possible to eliminate those spurious combinations of levels that could describe data at one particular energy, but could not produce a reasonable energy dependence for the matrix elements. We also note that fits to the data were attempted only when both $\sigma(\theta)$ and $P(\theta)$ data were available. It was possible to describe *either* of these data sets via a wide choice of levels at each energy, but good simultaneous fits to both data sets were sparse.

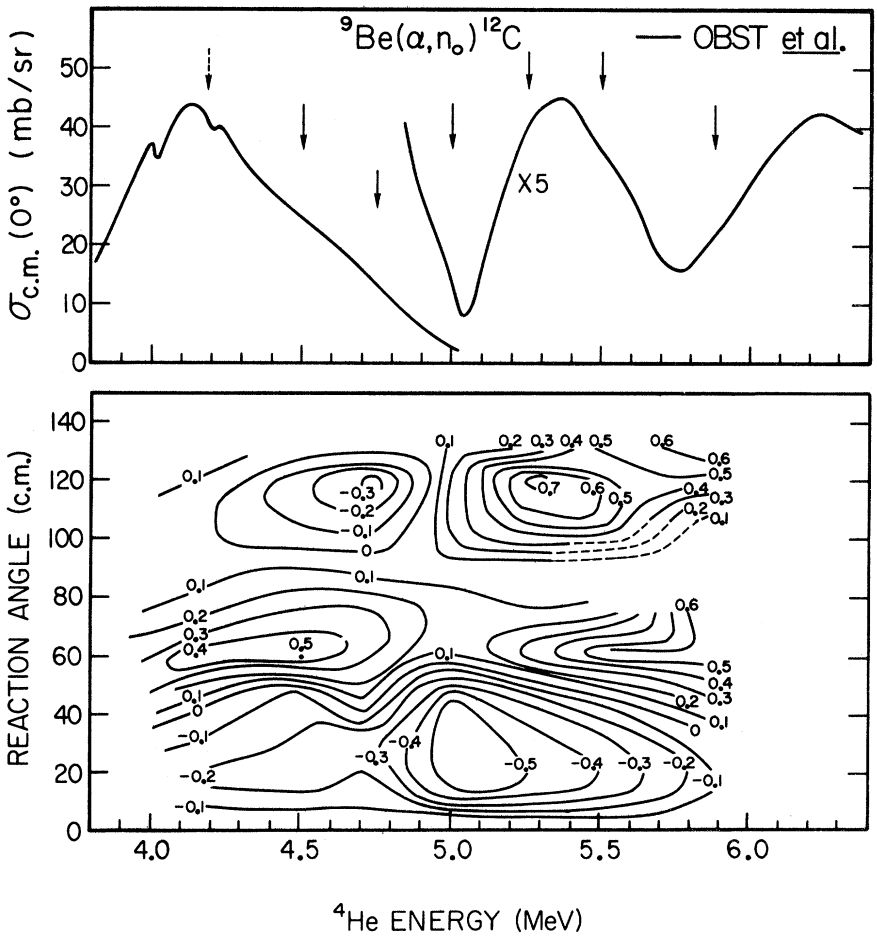

FIG. 5. A contour plot of the present neutron-polarization data for the g.s. neutron group. Above the plot a $\sigma(0°)$ excitation curve is sketched, using the data of Obst *et al.* The lines represent constant values of the polarization as a function of energy and angle and are shown in intervals of 0.1 of $P(\theta)$. The dashed lines are used when the data are insufficient to determine the trend of the contours.

The cross-section data used in the analysis were those recently published by Obst *et al.*[6] These authors reportedly eliminated the discrepancies in previous measurements on this reaction, particularly as regards to the absolute magnitude of the cross section. However, as the energies of measurement of $\sigma(\theta)$ and $P(\theta)$ differed, we used the closest energies for the two data sets, as labeled in the figures. Since the $\sigma(\theta)$ data were measured with considerably thinner targets than were the polarizations, the energies for $\sigma(\theta)$ are taken to be the energy at which the calculations were made, a choice which primarily influences the energy plot of the matrix elements below and, hence, to some extent the resonance energies that emerge.

The level assignments made in previous investigations were used as starting points for our calculations and consisted of those of Lietz, Trevino, and Darden[1,2] and those of Risser, Price, and Class.[3] Darden showed that the g.s. neutron $\sigma(\theta)$ and $P(\theta)$ data at 4.18 MeV could be adequately described by assuming that three broad states contributed to the reaction. Two of these states were associated with peaks in $\sigma(\theta)$ at 4.2 and 4.5 MeV and were assigned $J^\pi(l_\alpha)$ values of $\frac{5}{2}^+(1)$ and $\frac{3}{2}^+(3)$, respectively. (See note, Ref. 2.) A contribution from a $\frac{5}{2}^-(4)$ level was also noted. In addition to these assignments, Risser, Price, and Class had previously noted that a $\frac{1}{2}^-(2)$ and $\frac{7}{2}^-(2)$ pair of levels described their $\sigma(\theta)$ data in the same energy range equally well. In our calculations, both of these sets as well as numerous other likely combinations of levels were tried at various energies, but with little success. We do not expect to detect contributions from the narrow resonance ($\Gamma = 60$ keV) at $E_\alpha = 4$ MeV as our polarization data were recorded with targets much thicker than this level width. Following the analysis of the (α, α) elastic scattering data by Goss *et al.*[7] additional calculations were made to look for some of their findings, as commented upon below.

After an extensive search for many possible level combinations, it was found that one set of levels with $J^\pi(l_\alpha)$ assignments of $\frac{5}{2}^+(1)$, $\frac{3}{2}^+(3)$, $\frac{5}{2}^-(4)$, and $\frac{1}{2}^-(2)$ provided a superior fit to both the $\sigma(\theta)$ and $P(\theta)$ data over the entire energy range except at $E_\alpha = 4.75$ MeV where a number of different level combinations described the data as well or better than this set. The calculations using these J^π assignments are shown as the solid lines in Figs. 6–11, where it is seen that the magnitudes and

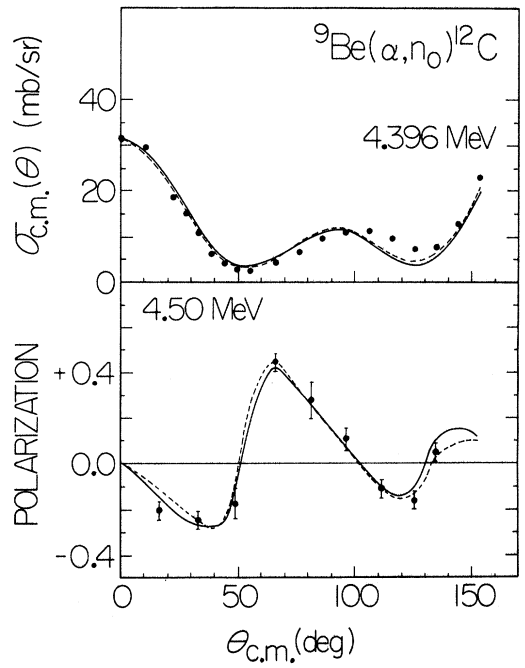

FIG. 6. The solid lines are the results of the *S*-matrix search code for the set of levels that provided the best over-all fit at all energies to the data (see text). The dashed lines include a $\frac{3}{2}^-(0)$ state substituted for a $\frac{5}{2}^-(4)$ state (which showed little amplitude at this energy in any case). The cross section data are those of Obst *et al.*

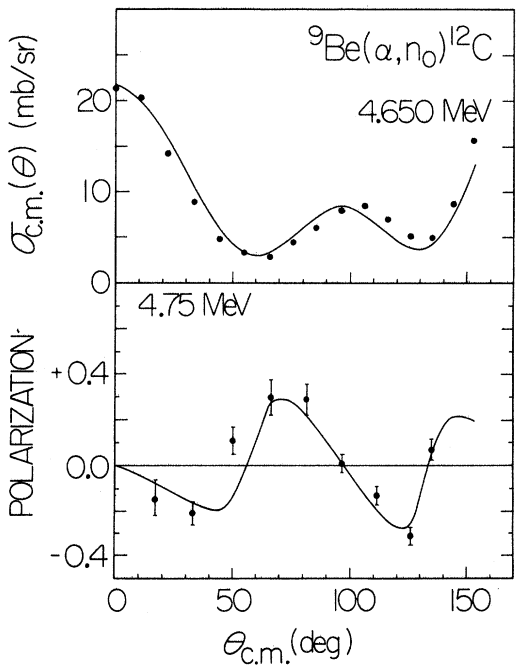

FIG. 7. The solid lines are the *S*-matrix search calculations with the best over-all set of level parameters (see text).

shapes of the $\sigma(\theta)$ and $P(\theta)$ data are generally well produced at all energies. In the following discussions, the E_α quoted are those at which $P(\theta)$ data were recorded. For $E_\alpha > 5$ MeV, no other sets of levels were found which could reproduce the data at any energy. At 4.75 MeV, several combinations of levels yielded fits equal to that shown, but these combinations failed to describe the data at neighboring energies. At 4.50 MeV numerous combinations of levels yielded equally good fits when two of the levels were $\frac{5}{2}^+(1)$ and $\frac{3}{2}^+(3)$. It was obvious that these two levels so dominated the reaction here that the inclusion of any third level yielded a better fit. Hence little insight into the properties of this third state is obtained. One of the combinations of levels that yielded an equally good fit to the data at 4.50 MeV had $J^\pi(l_\alpha)$ assignments of $\frac{5}{2}^+(1)$, $\frac{3}{2}^+(3)$, $\frac{1}{2}^-(2)$, and $\frac{3}{2}^-(0)$ and this fit is shown as the dashed line in Fig. 6. This will be discussed further below.

The squared amplitudes of the matrix elements for the $\frac{5}{2}^+$-$\frac{3}{2}^+$-$\frac{5}{2}^-$-$\frac{1}{2}^-$ set of levels are plotted in Fig. 12 vs E_α. The amplitudes exhibit a resonance-like behavior and suggest the presence of at least five states in this energy range, all of which are quite broad. Because the amplitudes do not generally attain the expected value of unity,

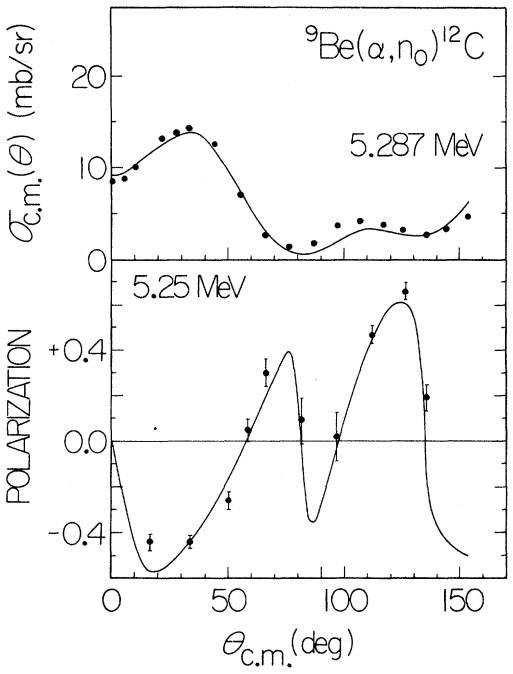

FIG. 9. The solid lines are the S-matrix search calculations with the best over-all set of level parameters (see text).

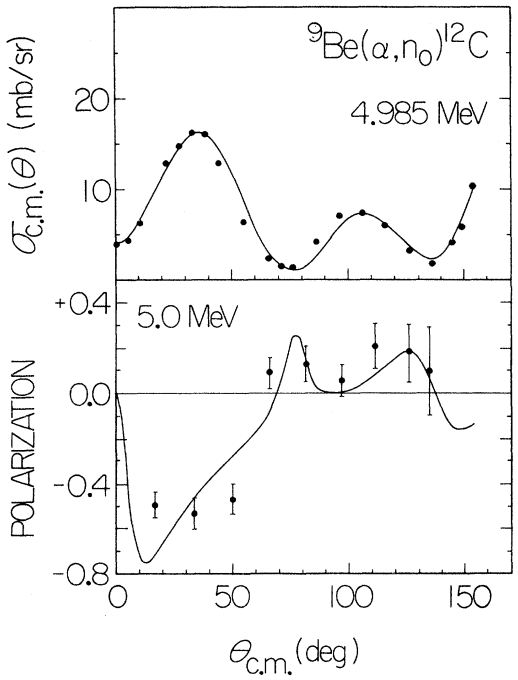

FIG. 8. The solid lines are the S-matrix search calculations with the best over-all set of level parameters (see text).

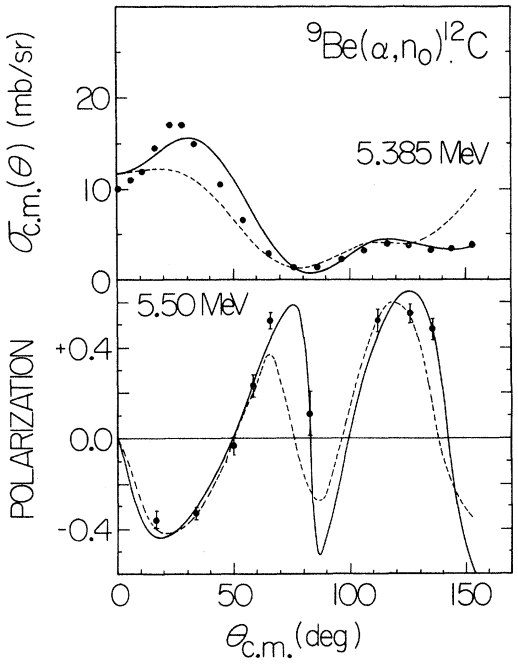

FIG. 10. The solid lines are the S-matrix search calculations with the best over-all set of level parameters (see text). The dashed lines were calculations where a $\frac{3}{2}^+(1)$ state was substituted for a $\frac{3}{2}^+(3)$ state in the calculations. The noticeably poorer fit here enabled us to exclude the possibility of a $l_\alpha = 1$ assignment for this state.

the precise determination of the resonance energy from Fig. 12 is difficult and one must rely on comparison of this figure with the 0° yield curve. The failure to attain the unity value for $|S^{J^\pi}|$ may only reflect the sparseness of the energies of measurement and/or may indicate that the matrix elements are energy averaged because the $P(\theta)$ data were measured with ~300-keV thick targets.

A comparison of the 0° yield curve for the (α, n_0) reaction with the matrix-element plot in Fig. 12 suggests that the resonances at 4.2 and 4.5 MeV have $J^\pi(l_\alpha)$ assignments of $\frac{3}{2}^+(3)$ and $\frac{5}{2}^+(1)$. As noted above, the fits to the data are improved somewhat when a third state is included in the calculations to presumably account for lower energy data. Although the data could be fitted equally well with a variety of J^π assignments for this third state (and hence we cannot distinguish among them in this work), the inclusion of a $\frac{3}{2}^-(0)$ state deserves special mention as the (α, α) analysis favors the presence of such a state at about 3.8 MeV. When this state is included in the calculations, the matrix elements for the $\frac{3}{2}^+$ and $\frac{5}{2}^+$ states are modified in the fitting process, with the net result being that the ordering of these two positive-parity states is reversed from that indicated by Fig. 12. This alternate ordering is the one used by Goss *et al.* in their (α, α) scattering calculations. As indicated in their paper, the region below $E_\alpha = 4$ MeV requires additional work as their data are not well reproduced. As their $\frac{3}{2}^-(0)$ assignment is only tentative at this time, the ordering of the positive-parity states is in doubt until more is known about the region just below $E_\alpha = 4$ MeV. As a final comment on these positive-parity states, we note that both states are well described under the assumption that they are formed by single l_α values. In particular, we note that the matrix element for the $\frac{3}{2}^+(1)$ assignment was always close to zero whenever it was included in the calculations, from which we conclude that this matrix element does not contribute to the (α, n_0) reaction. Although this may seemingly contradict some of the (α, α) results where both $l_\alpha = 1$ and 3 were noted to contribute for this state, Goss *et al.* comment that the contribution for a $\frac{3}{2}^+(1)$ state may only reflect the insensitivity of the α elastic scattering data to the J value and that the $l_\alpha = 1$ contribution in their analysis is attributed to the $\frac{5}{2}^+(1)$ state. The present analysis is of course sensitive both to l and J.

In Fig. 12, the presence of at least three states above $E_\alpha = 5$ MeV is noted. A $\frac{1}{2}^-(2)$ assignment

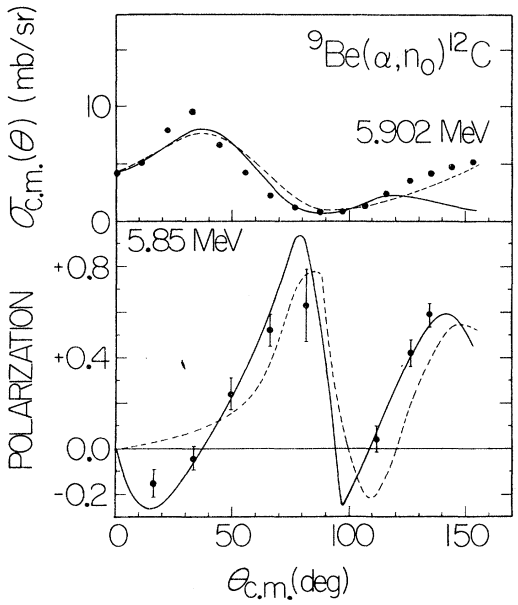

FIG. 11. The solid lines are the S-matrix search calculations with the best over-all set of level parameters (see text). The dashed lines were calculations where a $\frac{3}{2}^+(1)$ state was substituted for a $\frac{3}{2}^+(3)$ state in the calculations.

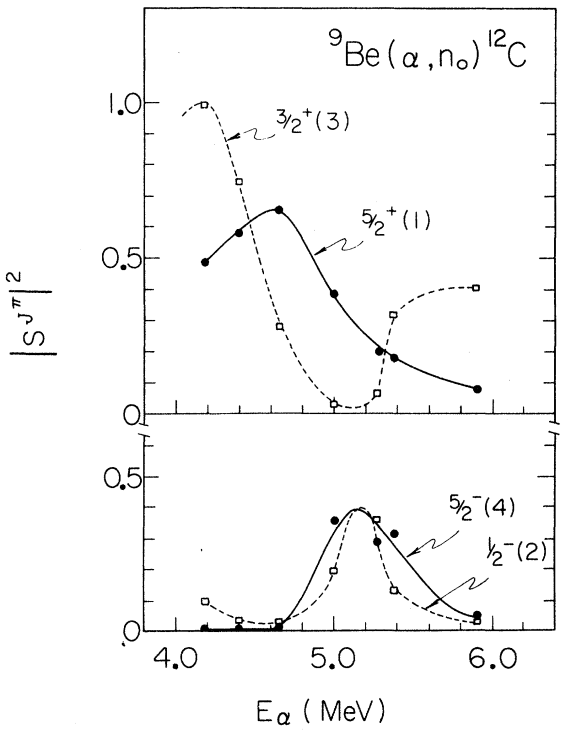

FIG. 12. A plot of the square of the amplitude of the single-energy S matrix elements derived as a result of fitting $\sigma(\theta)$ and $P(\theta)$ data at the individual energies. The lines sketched through the data points are only suggestive of what the resonance structure might look like (see text).

can be associated with the structure in the excitation curves near 5.3 MeV. Whether the $\frac{5}{2}^-(4)$ assignment is also associated with this same structure is not entirely clear. A prominent narrow resonance is observed in the (α, α), (α, n_1), and (α, n_2) reaction excitation curves at $E_\alpha = 5.0$ MeV, whereas the (α, n_0) data show a minimum in the 0° yield curve at this energy. As the width of the structure appears to be wider in the neutron channels than in the α elastic channel, more than one state may contribute near this energy. Goss *et al.* in fact note that two closely spaced states of opposite parity are required to explain their data near 5 MeV. Of the two possible pairs of states, one set consists of $\frac{5}{2}^-(4)$ and $\frac{7}{2}^+(3)$ assignments. The latter state has $\Gamma_\alpha \simeq \Gamma$ and, hence, probably contributes little to the neutron channel. The $\frac{5}{2}^-$ state has a fraction of the total width attributed to Γ_n. Now, in our analysis, the $\frac{5}{2}^-(4)$ matrix element is appreciable at 5 MeV, indicating that such a state may be present near this energy. However, the estimate of the width of this state from Fig. 12 indicates that it is much wider than that determined in the (α, α) analysis and its centroid is at a higher energy. What is actually taking place is not clear. It may be that two states of this configuration are present here which would explain the anomalous behavior of the $\frac{5}{2}^-(4)$ matrix element in Fig. 12. Alternatively, it may be that only a single $\frac{5}{2}^-(4)$ state located near 5.3 MeV is present. In this case, the alternate set of levels proposed in the (α, α) analysis (i.e., a $\frac{7}{2}^-$ state plus a $\frac{3}{2}^+$, $\frac{5}{2}^+$, or $\frac{7}{2}^+$ state) would most likely apply. Clearly, more work is required to clarify the structure here.

The third prominent matrix element evident for $E_\alpha > 5$ MeV in Fig. 12 is a $\frac{3}{2}^+(3)$ configuration. As noted in this figure, the energy trend of the matrix element for this state is not clear enough to correlate with the structure in the yield curves. That is, the (α, n_1) yield curve exhibits a resonance at ~5.7 MeV, but this is not evident in the other exit channels. A very broad resonance is observed in most exit channels near ~6.25 MeV. Both of these resonances are candidates for the $\frac{3}{2}^+(3)$ assignment. An extension of the present analysis to higher energy would require additional polarization data, since the nature and number of states contributing at higher energies is uncertain, and our work has shown that both data sets are required for rewarding calculations. The (α, α) work of Goss *et al.* is also of no aid here, as their analysis was primarily concerned with the structure up to $E_\alpha \simeq 5$ MeV. The level energy is tentatively assigned as $E_\alpha = 6.25$ MeV since structure in (α, n_0) is seen here, but clearly more work is required.

This $\frac{3}{2}^+$ state is also noted to be formed by a single l_α value of three units. For comparison, calculations made assuming $l_\alpha = 1$ for this state and shown as dashed lines in Figs. 10 and 11 result in noticeably poorer descriptions of the data. Although the $l_\alpha = 3$ assignment is seemingly inconsistent with the $l_\alpha = 1$ assignment made in the (α, α) work, the latter paper emphasizes that their assignment was included in the calculations as a background state to primarily fit the data near $E_\alpha = 5$ MeV. Furthermore, those authors state that no attempt was made to fit the data above $\simeq 5$ MeV because of the uncertain nature of the higher energy states. Those authors feel that because they do not describe the data above 5 MeV, there is no discrepancy with our assignments which do describe the neutron-reaction data.

V. SUMMARY OF THE REACTION CALCULATIONS

The ground-state neutron-cross-section and polarization data have been described over the entire 4- to 6-MeV energy interval by assuming the presence of at least five broad states in ^{13}C. A summary of the more prominent states deduced in this analysis is given in Table II. No level widths are quoted here as we do not feel that the data are complete enough to allow us to determine these reliably. The reader may obtain an estimate of these from Fig. 12. As we have conducted an extensive search for alternate sets of levels to describe the data (~400 separate calculations) with a null result, we believe that these assignments are

TABLE II. $J^\pi(l_\alpha)$ assignments and excitation energies in ^{13}C deduced from $^9Be(\alpha, n_0)$ reaction analyses.

E_α (MeV)	E_x (^{13}C) (MeV)	J^π	l_α	l_n
4.18	13.56	$\frac{3}{2}^+$ [a]	3	2
4.5	13.76	$\frac{5}{2}^+$ [a]	1	2
5.3	14.29	$\frac{1}{2}^-$	2	1
5.3 [b]	14.29	$\frac{5}{2}^-$	4	3
6.25 [c]	14.95	$\frac{3}{2}^+$	3	2

[a] The correlation of these J^π assignments with the resonance energies depends upon the states for $E_\alpha < 4$ MeV (see text).

[b] There is the possibility that this state is composed of two states of same J^π located at $E_\alpha \simeq 5$ and ~5.4 MeV.

[c] The correlation of the $\frac{3}{2}^+$ assignment with this energy is based on visual observation of the $^9Be(\alpha, n_0)$ excitation curve. It could be associated with a state corresponding to $E_\alpha \simeq 5.7$ MeV which is ***not*** apparent in the (α, n_0) reaction yield curves.

unique. The general agreement of the level assignments with those derived earlier by Lietz, Trevino, and Darden and now, in the completely separate type of analysis by Goss *et al.*, is gratifying. Although there are some discrepancies in the (α, α) and (α, n_0) analyses, they are all explainable and may be unreal. Such uncertainties are anticipated when the level structure is so broad and overlapping (as it is here) that not even the number of contributing states is known. An additional difficulty arises in correlating results for the different reaction channels, as the states appear to contribute selectively to some of the open exit channels. Finally, we note that although we have adopted the approach that only the compound-nucleus mechanism is important, there is certainly some direct-reaction-mechanism contribution here and the extent of its influence on the analysis is difficult to assess, although it is probably small for this channel.

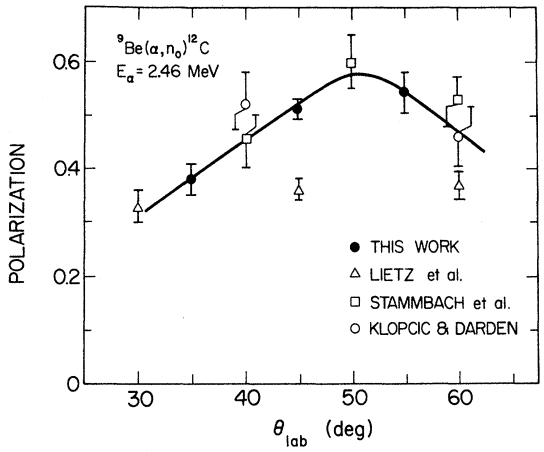

FIG. 13. A plot of all of the published data at $E_\alpha = 2.65$ MeV for the g.s. neutron group. The agreement between all of the recent measurements is good, so that the 45° point of Lietz *et al.* can probably be ignored.

VI. REACTION AS A SOURCE OF POLARIZED NEUTRONS

The large polarizations observed for both neutron groups in this work make them potentially useful sources of polarized neutrons in energy ranges not previously accessible to users of single-ended electrostatic accelerators. The figure of merit $(P^2\sigma/S)$ is taken to be the usual criterion[22] for determining the usefulness of the source, where $P = P(E, \theta)$ is the neutron polarization, $\sigma = \sigma(E, \theta)$ is the reaction differential cross section at the same energy and angle, and S is the atomic-stopping cross section. The latter is taken from Northcliffe and Schilling.[23] We have tabulated the most promising source conditions for each neutron group in Table III, clustering them according to the range of neutron energies over which they are useful. As is the case with many reactions, these sources are useful only over discrete energy ranges. The most useful regions for both neutron groups for these reactions occur for $E_\alpha \geq 5$ MeV; only at 5.5 MeV (15 and 30°) are both neutron groups simultaneously useful. In this table, we have also included our results for the g.s. neutron group at $E_\alpha = 2.65$ MeV; our data for this energy are compared with those of Lietz *et al.*[1] in Fig. 13 together with some more recent work.[17,24] The data of Lietz *et al.* are noted to be low principally at 45° near the peak in the polarization function. Hence, this reaction is more promising

TABLE III. The figures of merit $(P^2\sigma/S)$ of the ^{9}Be(α, n_0) and ^{9}Be(α, n_1) reactions as sources of polarized neutrons.

E_n (MeV)	E_α (MeV)	θ_{lab} (deg)	$\lvert P(\theta)\rvert$	$\sigma(\theta)$ [a] (mb/sr)	S [b] (10^{-15} eV cm^2)	$(P^2\sigma/S)$ (10^{-12} eV sr)
			^{9}Be$(\alpha, n_0)^{12}$C			
7.7–8.1	2.65	35–55	0.38–0.54 [c]	9.5–13.5	17.6	0.11–0.16
7.4–8.1	5.25–5.85	105–130	0.48–0.66	2.75–3.5	10.3–11.2	0.06–0.12
9.0	4.5	60	0.45	4.85	12.5	0.08
9.77	5.5	60	0.52	3.25	10.8	0.08
10.25–10.96	5.0–5.5	15–30	0.33–0.53	12.5–19.9	10.8–11.6	0.2–0.48
			^{9}Be$(\alpha, n_1)^{12}$C (4.43 MeV)			
3.35–3.95	4.5–5.5	90–120	0.23–0.36	16–23.5	10.8–12.5	0.1–0.18
4.0–4.5	4.5–5.5	75–105	0.24–0.34	19–23	10.8–12.5	0.1–0.2
6.1–6.4	5.5–5.85	15–30	0.14–0.20	51–85	10.3–10.8	0.16–0.23

[a] Taken from Ref. 6.
[b] Taken from Ref. 23.
[c] $P(\theta)$ values are published in Ref. 24 (errata).

than believed by Lietz *et al.* Recent work by members of the same group[24] has confirmed the higher values. Our data have been published in their work.[24]

To evaluate the over-all usefulness of this reaction, the figures of merit must be compared to those attained for other reactions. This is most easily done by referring to the recent comprehensive summary of Walter,[22] whose tabulated (and graphical) figures of merit are directly comparable to those given here. A quick perusal would seem to indicate that the present reaction fares poorly when compared to such well-established sources as the $T(p, n)$ and $D(d, n)$ reactions, as the figures of merit are 5 to 10 times lower for the (α, n) reaction. However, for single-ended electrostatic or small tandem accelerators ($E_{\text{proj}} \leq 6$ MV), the comparison becomes considerably more favorable. In this case, the latter reactions have maximum neutron energies of 4.6 MeV (at 33° lab) and ≃8 MeV (at 34° lab), respectively. The (α, n_0) therefore provides a new and important source of polarized neutrons in the 8- to 11-MeV energy range, a range not previously accessible to users of single-ended accelerators. Furthermore, the $^9\text{Be}(\alpha, n_1)$ reaction has a figure of merit that is comparable to that of the $D(d, n)$ reaction, so that it is competitive on this basis.

There are some advantages that favor the (α, n) reaction that should be taken into account. The beryllium targets, which are easily prepared by vacuum evaporation onto tungsten disks, are very stable, even under prolonged bombardment with beam currents of 15–20 μA. This may be contrasted to the $T(p, n)$ and $D(d, n)$ reactions both of which gain their favorable figure of merit through the use of gaseous targets.[22] The use of such targets frequently limits beam currents to ~1 μA, and hence, the (α, n) reaction gains a considerable advantage based on this factor. A second advantage arises in that the α-particle beam from the accelerator produces little or no neutron background with which the experimentalist must contend. This is not the case for the $D(d, n)$ reaction [the closest competitor to the $^9\text{Be}(\alpha, n)$ reaction] where the breakup neutrons can be a serious problem. Lastly, although there are several neutron groups emitted in the $^9\text{Be}(\alpha, n)$ reaction, the contributions from them may be easily separated using conventional fast electronics. In at least a few cases, polarization measurements for two different neutron energies can be recorded simultaneously by using the (α, n) reaction in the vicinity of $E_\alpha = 5.5$ MeV.

In summary, the $^9\text{Be}(\alpha, n)$ reaction provides very useful sources of polarized neutrons for various neutron-energy intervals throughout the 3.5- to 11-MeV range. The several experimental advantages associated with the use of these reactions should be considered in selecting the appropriate source for the specific experiment.

The authors are pleased to acknowledge Dr. George Marr who wrote the *S*-matrix search program used in this analysis and D. R. Sukis who constructed the motor generator control.

---

*Work supported in part by the National Science Foundation.

†Present address: Shell Development Company, Houston, Texas 77001.

‡Present address: Brun Corporation, Columbus, Ohio 43212.

[1]G. P. Lietz, S. F. Trevino, A. F. Behof, and S. E. Darden, Nucl. Phys. 67, 193 (1965).

[2]S. E. Darden, in *Proceedings of the Second International Symposium on Polarization Phenomena of Nucleons*, edited by P. Huber and H. Schopper (Birkhauser-Verlag, Basel, 1966), p. 433. The assignments noted in their Fig. 10 are correct. The ordering of the states in their text is incorrect.

[3]J. R. Risser, J. E. Price, and C. M. Class, Phys. Rev. 105, 1288 (1957).

[4]F. Ajzenberg-Selove, Nucl. Phys. A152, 1 (1970).

[5]W. L. Baker, C. E. Busch, J. A. Keane, and T. R. Donoghue, Phys. Rev. C 3, 494 (1971).

[6]A. W. Obst, T. B. Grandy, and J. L. Weil, Phys. Rev. C 5, 738 (1972).

[7]J. D. Goss, S. L. Blatt, D. R. Parsignault, C. D. Porterfield, and F. L. Riffle, following paper, Phys. Rev. C 7, 1837 (1973).

[8]P. Hillman, G. Stafford, and C. Whitehead, Nuovo Cimento 4, 67 (1950).

[9]G. L. Morgan, R. L. Walter, C. R. Soltesz, and T. R. Donoghue, Phys. Rev. 150, 830 (1966).

[10]T. R. Donoghue, W. L. Baker, P. L. Beach, D. C. De Martini, and C. R. Soltesz, Phys. Rev. 173, 952 (1968).

[11]C. R. Soltesz, D. C. De Martini, and T. R. Donoghue, Phys. Rev. C 4, 1015 (1971).

[12]D. R. Sukis, R. P. Sullivan, and T. R. Donoghue, Bull. Am. Phys. Soc. 11, 603 (1966); also D. R. Sukis, M.S. thesis, The Ohio State University, 1966 (unpublished).

[13]R. E. Shamu, Nucl. Instr. Methods 14, 297 (1961).

[14]C. R. Soltesz and T. R. Donoghue, Bull. Am. Phys. Soc. 12, 215 (1967).

[15]G. R. Satchler, L. W. Owen, A. J. Elwyn, G. L. Morgan, and R. L. Walter, Nucl. Phys. A112, 1 (1968).

[16]J. Atkinson and J. E. Sherwood, Nucl. Instr. Methods 34, 137 (1965).

[17]Th. Stammbach, G. Spalek, J. Taylor, and R. L. Walter, Nucl. Instr. Methods 80, 304 (1970).

[18]T. R. Donoghue, D. C. De Martini, C. R. Soltesz, and D. R. Sukis, Bull. Am. Phys. Soc. 11, 12 (1966); also,

Bull. Am. Phys. Soc. 12, 500 (1967).
[19]L. Van der Zwan and K. W. Geiger, Nucl. Phys. A152, 481 (1970).
[20]G. Marr, Ph.D. dissertation, The Ohio State University, 1968 (unpublished). (Available from University Microfilms.)
[21]T. A. Welton, in *Fast Neutron Physics Part II*, edited by J. B. Marion and J. L. Fowler (Interscience, New York, 1960), Chap. V F.
[22]R. L. Walter, in *Polarization Phenomena in Nuclear Reactions*, edited by H. H. Barschall and W. Haeberli (Univ. of Wisconsin Press, Madison, 1971), p. 317.
[23]L. C. Northcliffe and R. F. Schilling, Nucl. Data A7, 233 (1970).
[24]J. T. Klopcic and S. E. Darden, Phys. Rev. C 3, 2171 (1971); see also their errata Phys. Rev. C 4, 1494(E) (1971). Our ^{9}Be(α, n_0) data at $E_\alpha = 2.65$ MeV are published in their errata.

PHYSICAL REVIEW C VOLUME 7, NUMBER 5 MAY 1973

Elastic Scattering of α Particles by ^{9}Be and Highly Excited States of ^{13}C†

J. D. Goss,* S. L. Blatt, D. R. Parsignault,‡ C. D. Porterfield,§ and F. L. Riffle¶
Department of Physics, The Ohio State University, Columbus, Ohio 43210
(Received 22 December 1972)

The elastic scattering of α particles by ^{9}Be has been studied in the bombarding energy range of 1.7–6.2 MeV. 10 excitation functions in 50-keV steps and five angular distributions near 5 MeV were measured. The elastic scattering data in the 3.5–5.0-MeV region were analyzed with the compound-nucleus theory using a computer code which evaluates the cross section in the "single-level" approximation. Analysis in terms of seven resonances reproduces many of the features of the data. Tentative spin and parity assignments are given.

I. INTRODUCTION

The states of ^{13}C below the ^{9}Be + α separation energy (at 10.651 MeV) are relatively well known, having been investigated extensively both experimentally and theoretically.[1] However, in the region of excitation above this energy virtually no spin and parity assignments have been made and information concerning level widths and level positions is incomplete.[1,2] The reactions ^{9}Be$(\alpha, \alpha)^{9}$Be and ^{9}Be$(\alpha, n)^{12}$C can be used to investigate this region of ^{13}C, which appears as the compound nucleus in both reactions. Polarization measurements have been made on the latter reaction by De Martini, Soltesz, and Donoghue and are reported, together with an analysis of both polarization and (α, n) cross-section data, in the preceeding paper.[3]

In the present work, the region has been investigated through a study of elastic scattering of α particles by ^{9}Be. This reaction has previously been studied by Taylor, Fletcher, and Davis[4] who analyzed data taken above 9 MeV with an optical model but reported only fragmentary data below 9 MeV. In the present work, 10 excitation functions in the laboratory energy region of 1.7 to 6.2 MeV and five angular distributions between 5.0 and 5.5 MeV were measured. The fluctuations in the measured excitation functions are suggestive of compound-nucleus formation and the data were therefore analyzed with a compound-nucleus theory. Since most compound-nucleus analyses of elastic scattering data have been concerned with cases of spin-0 or spin-$\frac{1}{2}$ projectiles scattering from even-A nuclei, the present study entailed extensive calculations with a computer program especially written for this analysis. The results of the measurements and of these calculations are presented below.

II. EXPERIMENTAL PROCEDURE

The α-particle beam from the Ohio State University 6-MV Van de Graaff accelerator was magnetically analyzed to provide an absolute energy known to within ±5 keV. The beam was collimated by two slit boxes on the beam line and entered the chamber through a 1-mm-diam circular aperture. The beam was collected in a Faraday cup and measured with a Brookhaven Instrument Company precision current integrator. Typically, the beam currents used in the measurement of the data were 0.1 to 0.5 μA. The integrator was checked and found to be accurate to ±0.2% for this current range. It was also determined that for the charge collection geometry employed, electrostatic or magnetic suppression was not necessary.

The elastically scattered particles were measured simultaneously at four angles, using silicon surface-barrier detectors (with 300-μm depletion depths) mounted in a 23-in.-diam scattering chamber. The platform on which the detectors and